Toxicon 227 (2023) 107091

Contents lists available at ScienceDirect

Toxicon

journal homepage: www.elsevier.com/locate/toxicon

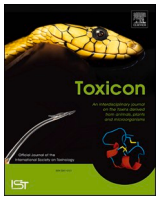

Toxic effects of the cylindrospermopsin and chlorpyrifos combination on the differentiated SH-SY5Y human neuroblastoma cell line

María G. Hinojosa [a], Daniel Gutiérrez-Praena [a,*], Sergio López [b,c], Ana I. Prieto [a], Francisco J. Moreno [b], Ángeles Jos [a], Ana M. Cameán [a]

[a] Área de Toxicología, Facultad de Farmacia, Universidad de Sevilla, C/ Profesor García González 2, 41012, Sevilla, Spain
[b] Área de Biología Celular, Facultad de Biología, Universidad de Sevilla, Avda. Reina Mercedes S/n, 41012, Sevilla, Spain
[c] Instituto de Biomedicina de Sevilla (IBiS), Hospital Universitario Virgen Del Rocío/CSIC/Universidad de Sevilla, 41012, Sevilla, Spain

ARTICLE INFO

Handling Editor: Ray Norton

Keywords:
Cylindrospermopsin
Chlorpyrifos
SH-SY5Y cells
Acetylcholinesterase activity
Cytotoxicity
Emerging contaminants

ABSTRACT

Due to climate change and anthropogenic activities, the levels of pollution of aquatic and terrestrial environments have increased in the last decades. In this sense, the rise of cyanobacterial blooms, which release secondary metabolites with toxic properties, and the global use of pesticides for agricultural purposes have a negative impact on ecosystems. Thus, it would be interesting to study the concomitance of both types of toxicants in the same sample, since it is possible that they appear together. The aim of the present work was to state the effects of the interaction between the cyanotoxin cylindrospermopsin and the pesticide chlorpyrifos in differentiated SH-SY5Y neuronal cells to assess how they could affect the nervous system. To this end, cytotoxicity, morphological, and acetylcholinesterase activity studies were performed during 24 and 48 h. The results revealed a concentration-dependent decrease in viability and interaction between both toxicants, together with clear signs of apoptosis and necrosis induction. In this sense, different stages on the differentiation process would lead to differences in the toxicity exerted by the compounds both isolated as in combination, which it is not observed in non-differentiated cells. Additionally, the acetylcholinesterase activity appeared not to be affected, which is a clear difference compared to non-differentiated cells. These results show the importance of studying not only the toxicants themselves, but also in combination, to assess their possible effects in a more realistic scenario.

1. Introduction

Cylindrospermopsin (CYN) is a cyanotoxin consisting of an alkaloid structure with a tricyclic guanidine coupled with a hydroxylmethyl uracil group, being a zwitterionic molecule and, thus, highly water-soluble and persistent (Chiswell et al., 1999; Falconer and Humpage 2006). These features have led to the detection of levels up to 1050 μg/L CYN in water reservoirs (Australia), while concentrations up to 97 μg/L have also been detected in drinking water (Guzmán-Guillén et al., 2015; WHO, 2020; Wörmer et al., 2010; Yang et al., 2021). In this sense, R. raciborskii, a known CYN-producer cyanobacterial species, and CYN were involved in human poisoning due to the use of contaminated water in Australia (Queensland) and Brazil (Caruaru) (Carmichael et al., 2001; Hawkins et al., 1985). The two most described mechanisms of action for CYN are inhibition of protein synthesis and GSH synthesis. Additionally, an increase in reactive oxygen species (ROS) production, apoptosis, or DNA damage, both in vitro and in vivo, has also been described (Pichardo et al., 2017). Furthermore, metabolic activation of CYN by the enzymatic complex cytochrome P-450 has shown to induce genotoxicity (Gura et al., 2011). This cyanotoxin is classified as cytotoxic, being the liver its main target; although CYN can exert damage at other levels as well, being the nervous system one of them (Buratti et al., 2017; Hinojosa et al., 2022). Although different routes of exposure have been reported, the ingestion of contaminated water or food has been described as the most important.

Together with the increase in CYN-producing blooms, the pollution of aquatic reservoirs by agricultural and livestock activities has also raised public concerns (Hassaan and Menr 2020). Among these compounds, pesticides, and especially organophosphates (OP) are some of the most used because of their balance effectiveness-toxicity in target and nontarget organisms (Ali et al., 2014; Aswathi et al., 2019). In most cases, their toxicity is due to their main mechanism of action,

* Corresponding author.
E-mail address: dgpraena@us.es (D. Gutiérrez-Praena).

https://doi.org/10.1016/j.toxicon.2023.107091
Received 30 January 2023; Received in revised form 8 March 2023; Accepted 20 March 2023
Available online 23 March 2023

irreversible inhibition of acetylcholinesterase activity (Worek et al., 1998). Among the OP, the most widely used and found in environmental samples is chlorpyrifos (CPF) (John and Shaike 2015).

Chlorpyrifos (O,O-diethyl-O-3,5,6-trichloro-2-pyridyl phosphorothioate) is a broad-spectrum OP insecticide that has been widely used in variable pest control situations. Its relevance is based on its low cost, persistence, toxicity, and wide applicability. For this, CPF levels have been detected in nearly 100 countries, applying to 8.5 million acres of crops per year (Koly and Khan, 2018). In this regard, CPF has been found in many environmental samples that range from rivers and freshwater lakes to snow, ice, or even artic regions (Watts, 2012). However, many studies point out its capacity to cause toxicity in different organisms, including humans, acting mainly as a neurotoxicant (Rahman et al., 2021). Thus, in January 2020, the Standing Committee on Plants, Animals, Food, and Feed of the EFSA decided not to renew the approval of CPF in the EU as a plant protection product. In this sense, "experts concluded that there are concerns related to human health, particularly in relation to possible genotoxicity and developmental neurotoxicity" in several experimental models (EFSA 2019; European Commission 2020). However, this compound can persist for several days in crops, varying its half-life according to the type of plant, going up to 120 days, depending on the environmental conditions (John and Shaike 2015; Lu et al., 2014). During this period, it can be absorbed through all routes, including inhalation, ingestion, and dermal absorption by different organisms, such as algae, fish, crustaceans, molluscs, insects, birds, livestock, and plants, that have demonstrated their ability to bio-accumulate this pesticide (Huang et al., 2020; Yurumez et al., 2007). The consumption of these products by humans and the associated risks have led EFSA to its decision.

The coexistence of pesticides and cyanobacterial products has been widely demonstrated in several environments (Metcalf and Codd 2020). Some fertilizers are known to stimulate the formation of cyanobacterial blooms and the use of soil containing cyanobacteria, fertilizers, and pesticides is a common practice in agriculture (Hercog et al., 2020; Wang et al., 2017). The different scenarios where both CYN and CPF can coexist increase the relevance of studying the effects of the combination, as several studies have reported relevant differences in the toxicological effects of many toxicants when isolated and in combination (Metcalf and Codd 2020). Regarding this, different reports have shown that both CYN and CPF have neurotoxic effects in different experimental models, mainly affecting acetylcholinesterase activity, and the synaptic function when studied in isolation (Eaton et al., 2008; Hinojosa et al., 2019a, 2019b, 2022). However, to our knowledge, there is only one study that uses the combination of both toxicants in vitro neuronal models (Hinojosa et al., 2020). In this study, it was indicated that the combination of CYN and CPF induced a reduction in GSH levels, an inhibition of AChE activity, cell death in non-differentiated neuroblastoma SH-SY5Y cells. Compared to CYN and CPF alone, the combination of each compound was antagonistic. However, cell differentiation has been described to be related to changes in metabolism and function that could lead to different responses to similar cellular stressors (Schneider et al., 2011). For this all, the aim of the present work is to assess the toxic effects of the CYN and CPF combination in differentiated SH-SY5Y cells for first time.

2. Materials and methods

2.1. Supplies and chemicals

CYN (purity >95% by HPLC) (ALX-350-149-M001) was purchased from Enzo Life Sciences. Minimum essential medium (MEM) (21,090-022), L-Glutamine (25030024), penicillin-streptomycin (15140122), pyruvate (11360039), non-essential amino acids (11140035), trypsin (25300054), PBS (P4417-100TAB), and fetal bovine serum (FBS) (10270106) were obtained from Gibco (Biomol, Sevilla, Spain). Acetylthiocholine iodide (ATCh) (A5751), the Bradford Reagent (B6916), 5,5′-Dithiobis (2-nitrobenzoic acid) (DTNB) (D8130), Chlorpyrifos (45,395), Nutrient Mixture F-12 Ham (N4888), retinoic acid (RA) (R2625), and brain-derived neurotrophic factor human (BDNF) (B3795) were purchased in Sigma-Aldrich (Madrid, Spain). The Cell Titer 96® AQueous One Solution Cell Proliferation Assay (CAS G3582) was obtained from Promega (Biomol, Sevilla, Spain).

2.2. Experimental cellular model system

The human neuroblastoma SH-SY5Y cell line is a subline of the SK-N-SH cell line obtained from a metastatic neuroblastoma. Among the different features of this differentiated cell line, their morphology, like primary cultures, the decrease in their proliferation rate and the increased expression of neuron-specific markers make of this cell line an interesting choice to study different diseases such as Parkinson or Alzheimer's (Gordon et al., 2013). This cell line was obtained from the ATCC collection (CRL-2266). Cells were maintained in 5% CO2 and 95% relative humidity at 37 °C (CO2 NuAire®, Spain). Medium (MEM and F-12) (1:1) was supplemented with 10% FBS, 1% sodium pyruvate, 1% non-essential amino acids, 1% penicillin/streptomycin solution, and 1% L-glutamine 200 mM. Cells were grown near confluence in 75-cm2 plastic flasks and harvested twice per week with 0.25% trypsin-EDTA (1X).

2.3. Cell differentiation

SH-SY5Y cells differentiation was carried out according to Hinojosa et al. (2019b). Briefly, the cells were seeded out at 500 cells/mL in plates of 48 wells to leave more space for differentiation. After 48 h, the medium was exchanged for differentiation medium containing FBS (1%), retinoic acid (10 μl), and BDNF (50 ng/ml). The medium was again changed and replaced by new differentiation medium after 48 h 2 twice more, and the cells were exposed after a week of differentiation. Then, this process was evaluated by morphological analysis.

2.4. Exposure of compounds individually and combined, and isobologram method

Stock solutions of 1 mg/ml CYN and 50 mg/ml CPF were prepared in sterilized milliQ water and absolute ethanol, respectively. Both solutions were maintained at −20 °C until their use.

For the cytotoxicity assays, serial dilutions of CPF were prepared in medium without serum (0, 25, 50, 75, 100, 125, and 150 μg/ml CPF).

For the combinational studies, the concentrations chosen were 0.075:8.5, 0.15:17, and 0.3:34 μg/ml CYN:CPF, following the results obtained of the most sensitive cytotoxicity biomarker after 24 h (in this case, MTS). The isobolograms method was applied according to Tatay et al. (2014). The CalcuSyn (Biosoft, Cambridge, UK) software calculated the combination index (CI) of the mixtures automatically. Thus, synergism ($CI < 1$), additivity ($CI = 1$), or antagonism ($CI > 1$) of the combinations could be elucidated.

2.5. Cytotoxicity assays

After replacing the growing medium, differentiated cells were exposed after a week from the start of the differentiation process in 48-well plates. Exposure solutions were added to the plates, and cells were incubated at 37 °C (5% CO_2 and 95% relative humidity) for 24 and 48 h. Vehicle control (ethanol) and a negative control (medium without serum) were also included.

The basal cytotoxicity endpoints assayed were protein content (PC) and tetrazolium salt reduction (MTS). All the assays were performed by triplicate.

The total protein content (PC) was quantified according to Bradford (1976) with some modifications (Pichardo et al., 2007). Briefly, the cells were exposed to 200 μl 0.1 N NaOH for 2 h and the Bradford reagent was

added afterwards. The absorbance was read at 620 nm.

The MTS reduction assay was evaluated in agreement with Baltrop et al. (1991). Briefly, 30 µl of the MTS solution were added to the cells in the differentiation medium after 24 or 48 h of exposure to the compounds, and the absorbance was measured at 490 nm after 3 h of incubation.

2.6. Acetylcholinesterase (AChE) activity determination

Acetylcholinesterase activity was measured following the procedures described by Ellman et al. (1961) and the modifications of Santillo and Liu (2015). Differentiated SH-SY5Y cells were exposed for 24 h to the same concentrations as for the combinational studies in the isobologram method. After this, 200 µl of 0.5 mM 5,5-dithio-bis-(2-nitrobenzoic acid) and 100 µM acetylthiocholine were added to each well, and the absorbance was measured at 410 nm every 90 s up to 1 h. A positive control consisting of a solution of 0.015 µg/ml parathion was used. All the assays were performed by triplicate.

2.7. Flow cytometry

Apoptosis and necrosis were assessed using a Vybrant Apoptosis Assay Kit # 2 (Molecular Probes, Barcelona, Spain) following the procedure previously described (Vermes et al., 1995; Jaramillo et al., 2010). This test uses Annexin V conjugated to Alexa Fluor 488 and propidium iodide (PI) to discriminate between intact cells (Annexin V−/PI−), apoptotic cells (Annexin V +/PI −) and necrotic cells (Annexin V +/PI +). Briefly, differentiated SH-SY5Y cells were exposed for 24 h to the EC_{50} of CYN and CPF. Then, apoptotic cells and necrotic cells were analyzed using a MACSQuant® VYB flow cytometer (Miltenyi Biotec) with an excitation wavelength of 488 nm and filters of 525/50 nm (B1) and 593–650 nm (B2) for detection of Alexa Fluor 488 and PI, respectively. The number of events considered were 10,000. The data were analyzed using MACSQuantify™ Software (Miltenyi Biotec).

2.8. Morphology

For the morphological studies, light microscopy, phase-contrast microscopy, and electron microcopy were used. The EC_{50} values after 24 h of exposure of CYN and CPF along with the fractions $EC_{50}/2$ and $EC_{50}/4$ were used for these assays. The procedures used are described in Hinojosa et al. (2019b).

2.9. Calculations and statistical analysis

Data were presented as mean ± standard deviation (SD) in relation to control. Statis-tical analysis was carried out using analysis of variance (ANOVA) followed by Dunnett's or Tukey's multiple comparison test (GraphPad InStat software, La Jolla, USA). Differences were considered significant from $p < 0.05$. The EC_{50} values were obtained by linear regression in the concentration-response curves.

3. Results

3.1. Cytotoxicity of CPF

After the exposure to 0–150 µg/ml CPF for 24 and 48 h of the differentiated SH-SY5Y cells, a concentration-dependent decrease of viability was observed (Fig. 1). The EC_{50} values obtained after 24 h were 33.51 ± 0.41 µg/ml (MTS) and 130.91 ± 1.75 µg/ml (PC). After 48 h of exposure, the EC_{50} values were 43.31 ± 0.99 µg/ml (MTS) and 46.52 ± 6.62 g/ml (PC). Thus, the MTS assay demonstrated to be the most sensitive biomarker.

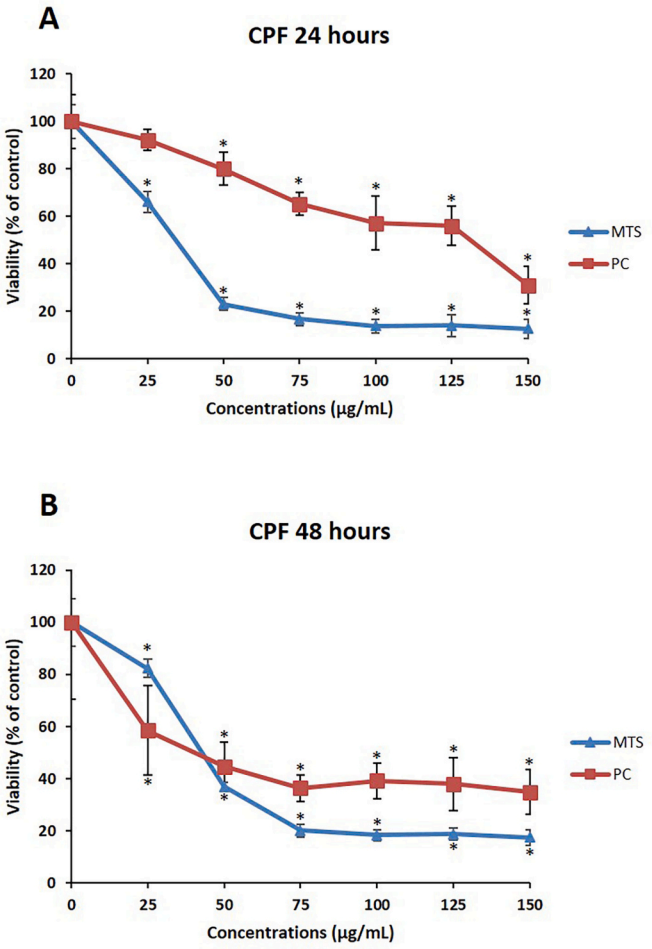

Fig. 1. Reduction of tetrazolium salt (MTS) and protein content (PC) on differentiated SH-SY5Y cells after 24 (a) and 48 h (b) of exposure to 0–150 µg/ml CPF. All values are expressed as mean ± s.d. * Significantly different from control group ($p < 0.01$).

3.2. Cytotoxic effects of the CYN-CPF combinations by the isobolograms method

Using the EC_{50} value for CYN obtained in a previous work (Hinojosa et al., 2019b), the exposure concentrations of CYN used were 0.075, 0.15 and 0.3 µg/ml CYN. Similarly, the CPF concentrations selected were 8.5, 17 and 34 µg/ml. Both compounds were used in a combined ratio of 0.3:34 and differentiated SH-SY5Y cells were exposed for 24 and 48 h (Table 1).

The experiments performed in the cells exposed to the combination for 24 h presented a combination index CI > 1 at the lowest concentrations, meaning an antagonistic response. However, the highest ones presented a synergic response (CI < 1) (Fig. 2a). Nonetheless, the response of the cells after 48 h exposure to the combination CYN-CPF was the opposite, occurring a synergic response at the lowest concentrations (CI < 1) while at the highest, an antagonistic response (CI > 1) was observed (Fig. 2b).

3.3. Acetylcholinesterase (AChE) activity determination

Neither of the concentrations tested caused significant differences with respect to the control group when the AChE activity was evaluated (Fig. 3).

Table 1
The parameter m, Dm and r are the antilog of x-intercept, the slope and the linear correlation coefficient of the median-effect plot, which signifies the shape of the dose-effect curve, the potency (IC_{50}), and the conformity of the data to the mass-action law, respectively. Dm and m values are used for calculating the CI value CI < 1, indicates synergism (Syn); CI = 1, indicates additive effect (Add); CI > 1, indicates antagonism (Ant). IC_{50}, IC_{75} and IC_{90} are the doses required to inhibit proliferation 50, 75 and 90%, respectively. CalcuSyn software provide automatically the IC_{50}, IC_{75} and IC_{90} values. Results of the potency are given as mean ± sd.

Toxicant	Time (h)	Dm (μg/mL)	m	r	CI values		
					CI_{50}	CI_{75}	CI_{90}
CYN	24 h	0.26632	0.6828 ± 0.1732	0.96930	N/A	N/A	N/A
	48 h	0.17057	1.8713 ± 0.6526	0.94423	N/A	N/A	N/A
CPF	24 h	7.52529	1.0199 ± 0.0202	0.99980	N/A	N/A	N/A
	48 h	23.87660	2.8477 ± 0.5275	0.98327	N/A	N/A	N/A
CYN + CPF	24 h	11.92411	1.6985 ± 0.1322	0.99698	1.980 ± 0.1349 Ant	1.181 ± 0.1091 Ant	0.728 ± 0.0922 Syn
	48 h	13.56687	1.1457 ± 0.0621	0.99854	1.270 ± 0.1645 Ant	2.026 ± 0.3855 Ant	3.264 ± 0.9239 Ant

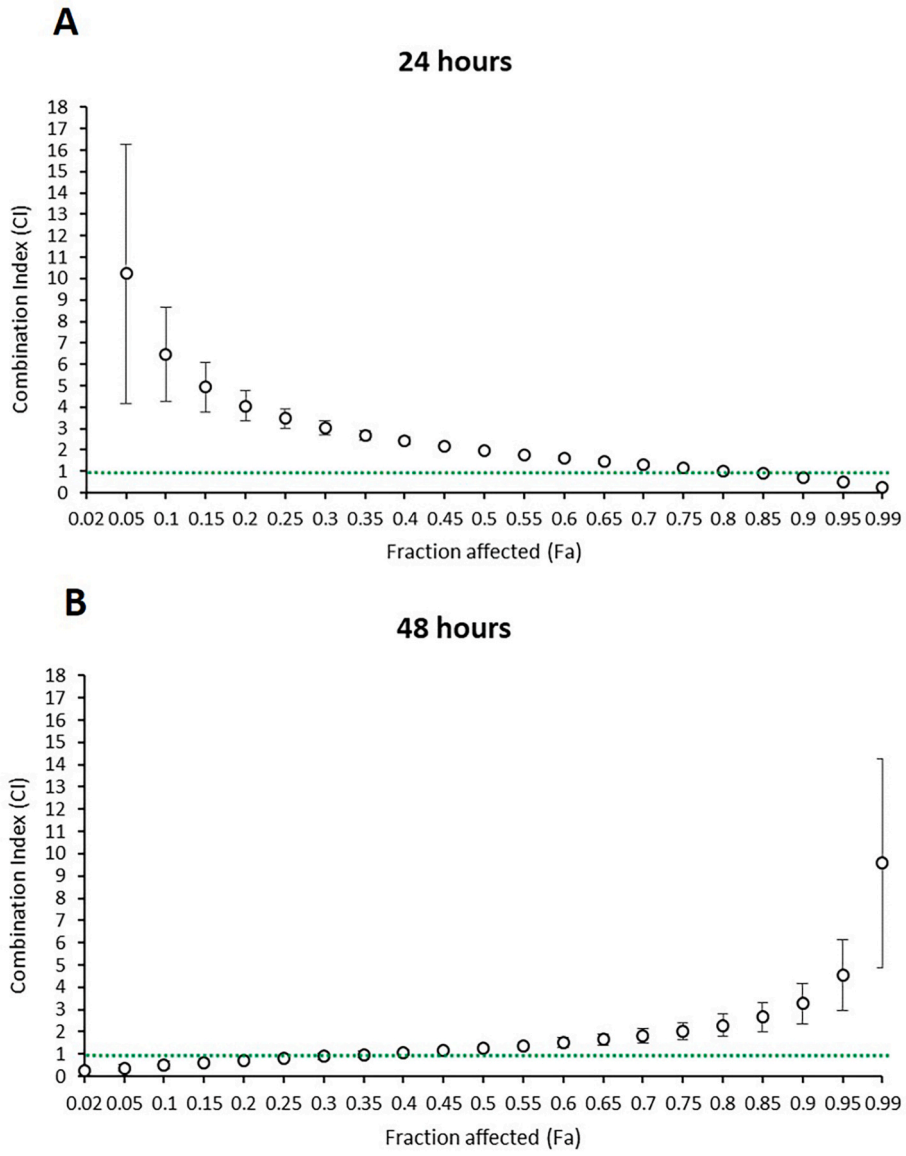

Fig. 2. Combination index (CI)/fraction affected (Fa) curve in SH-SY5Y cells exposed to CYN-CPF combination after 24 h (a) and 48 h (b) of exposure. Each point represents the CI ± s.d. At a fractional effect. The dotted line (CI = 1) indicates additivity, the area under the dotted line points out a synergist effect (CI < 1), and the area above the dotted line signifies antagonism (CI > 1).

3.4. Flow cytometry

Differentiated SH-SY5Y cells exposed to EC_{50} of CYN, CPF or CYN-CPF for 24 h underwent cell damage because of increased apoptosis and necrosis compared to control cells as visualized by Annexin V/PI staining assay (Fig. 4). The combination of CYN and CPF induced a

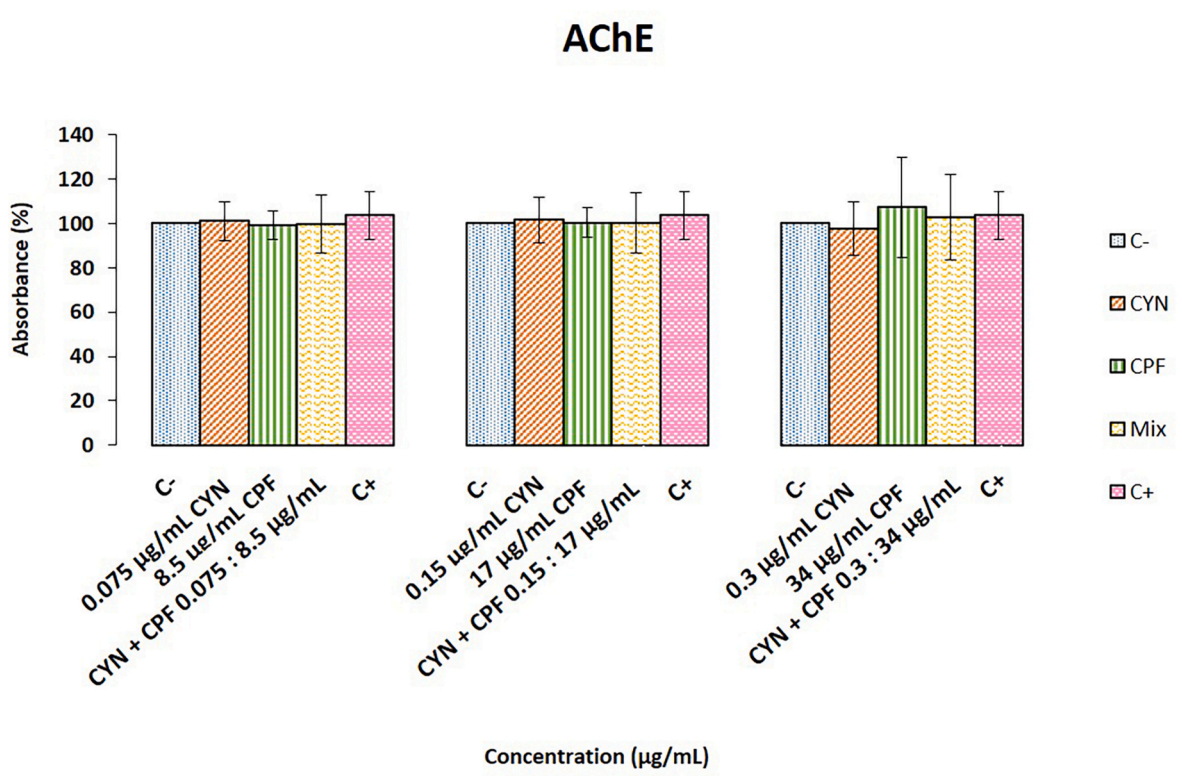

Fig. 3. Acetylcholinesterase activity (AChE) after 24 h in differentiated SH-SY5Y cells exposed to CYN (0–0.3 µg/ml), CPF (0–34 µg/ml) or CYN-CPF (same concentrations as isolated in the ratio 0.3:34). A solution of 0.015 µg/ml parathion was used as positive control (C+). All values are expressed as mean ± s.d.

higher percentage of apoptosis compared to CYN (Fig. 4a). There were no differences in the percentage of necrosis between the treatments (Fig. 4b).

3.5. Morphology

Unexposed differentiated SH-SY5Y cells frequently presented two types of morphology. The first type has a star shape, with cytoplasmatic projections that interact with neighbor cells (Fig. 5A). The second type presented spindle cells with scarce cytoplasmatic projections (Fig. 5A). In addition, cell division can be observed under a light microscope, with numerous cells in mitotic phase (Fig. 5B). The electron microscopy observations showed a rough endoplasmic reticulum (RER) with sharply delineated vermiform strands, a normal oval or spherical nucleus and intact nucleoli (Fig. 5C) surrounded by cytoplasm with unaltered mitochondria with recognizable cristae (Fig. 5C and D).

3.5.1. Microscope observations of cells exposed to CPF

Cells exposed to CPF showed a direct relationship between the concentration of exposure and the morphological alterations observed, which lead to cell death. No significant morphological alterations were observed after the exposure to the lowest concentration assayed (8.5 µg/ml CPF) compared to the control group. Cells exposed to 17 µg/ml CPF presented a lower cell density. In this regard, cell death was observable, although the proliferative ability was still active (Fig. 6B). Ultrastructurally, cells presented dilatations of RER with ribosomes still attached to cisternae (Fig. 6C), mitochondrial swelling with some identifiable cristae (Fig. 6D) and nucleus with nucleoli in segregation processes of the fibrillary and the granular components (Fig. 6E).

After exposure to the highest concentration assayed (34 µg/ml CPF), cell death signs (Fig. 7A and B) and apoptosis (Fig. 7D) were observed under phase-contrast, light, and electronic microcopy. At a cytoplasmic level, there was an increase in the number and size of heterophagosomes (Fig. 7C). In addition, nuclei presented heterochromatin aggregates and nucleoli showed segregated fibrillary and granular components (Fig. 7D).

3.5.2. Microscope observations of cells exposed to the combination CYN: CPF

Concerning the combinations, no significant morphological alterations were observed at the lowest combination concentrations assayed (0.075:8.5 µg/ml, CYN:CPF) with respect to the control group (Fig. 8A). At the medium concentration assayed (0.15:17 µg/ml, CYN:CPF), apoptotic features of condensed nuclei appeared, although cell division was also appreciable (Fig. 8B). Under electronic microcopy, cells presented dilated RER membranes with ribosomes attached to cisternae (Fig. 8C). In addition, nuclei showed nucleoli with all the components segregated (fibrillary and granular) (Fig. 8C and D).

At the highest combination concentration assayed (0.3:34 µg/ml, CYN:CPF), an intense decrease in cell density was observed, appearing numerous cell debris (Fig. 9A and B). At light microscopy, cells in different apoptosis stages were observed (heterochromatin condensation, apoptotic bodies formation) (Fig. 9C). Under electron microscopy, a high percentage of cells presented heterochromatic nuclei and intense membrane alterations, being these compatible with necrotic damage (Fig. 9D and E).

4. Discussion

The importance of studying toxicants as found in nature has been demonstrated, as chemicals can change their toxic properties depending on the characteristics of their surroundings (Walker 1998). In this sense, pesticides and cyanobacterial products have demonstrated to coexist in both aquatic and terrestrial scenarios, being able to interact (Singh et al., 2018). Among all of them, CYN and CPF are some of the most common and toxic substances found in aquatic environments (Hinojosa et al., 2020).

As Kovalevich and Langford (2013) described, neuronal

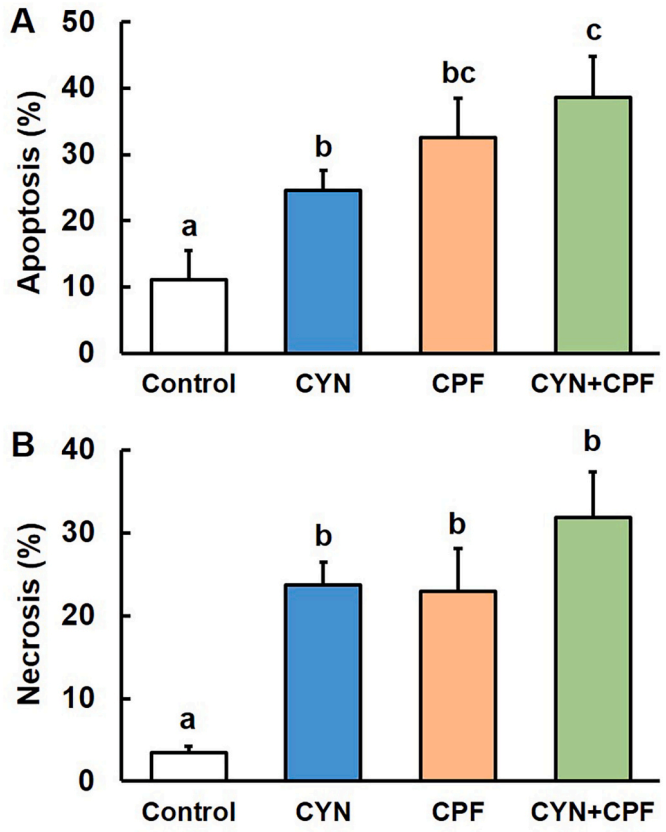

Fig. 4. Induction of apoptosis (a) and necrosis (b) on differentiated SH-SY5Y cells after 24 h of exposure to EC50 concentrations of CYN, CPF or CYN + CPF. The experiments were performed in triplicate and all values are expressed as % of total cells (mean ± s.d). Bars showing a different letter are statistically different ($p < 0.05$).

differentiation involves a cascade of events such as the formation and extension of neuritic processes and functional synapses, increased electrical excitability, and induction of neuron-specific enzymes, receptors, and neurotransmitters, among others. In contrast, the undifferentiated cell line continues to proliferate and expresses immature neuronal markers, but not mature ones. Therefore, the differentiation process leads SH-SY5Y cells to become morphologically more like primary neurons, which is interesting in our study to clarify the mechanisms by which both toxicants could induce toxicity.

In general, OP insecticides have demonstrated to induce neurotoxic effects in different cell lines such as SH-SY5Y, PC-12 or primary cultures, among others (Tiffany-Castiglioni et al., 2006). In the present study, the pesticide CPF showed a concentration-dependent decrease of the viability on the neuronal SH-SY5Y cell line, showing an EC_{50} value of CPF for this parameter (MTS, 24 h). These results agree with those obtained by Park et al. (2013), who reported the same concentration-dependent response in undifferentiated SH-SY5Y cells exposed to 0–200 μM CPF after 24 h of exposure, obtaining an EC_{50} value ~70 μg/ml. Furthermore, Raszewski et al. (2015) reported a time- and concentration-dependent viability response in undifferentiated SH-SY5Y cells exposed for 24, 48, and 72 h to 0–175 μg/ml CPF, providing an EC_{50} value after 24 h of ~100 μg/ml CPF. Similarly, Hinojosa et al. (2020) obtained 84 μg/ml CPF as the EC_{50} value in the MTS assay after the same time of exposure, also observing a concentration- and time-dependent response for CPF in undifferentiated SH-SY5Y cells. To our knowledge, this is the first report studying the cytotoxic effects of CPF in the differentiated SH-SY5Y cell line after 24 and 48 h of exposure. In this sense, the discrepancy between the results in undifferentiated and differentiated cells could be due to the different characteristics of both states of cell differentiation, as differentiated cells are more mature, more like primary neurons, and they express different neuronal markers than can be affected after exposure to this pesticide (Kovalevich and Langford 2013). Furthermore, the capacity of CPF to reduce viability has not only been demonstrated in this undifferentiated cell line, as Zurich et al. (2004) demonstrated its effect on GABAergic neurons, also causing a concentration-dependent response, obtaining significant changes from 3.5 μg/ml. In the present study, cell death signs were also corroborated by the morphological studies, being the findings qualitatively very similar to those observed in undifferentiated cells (Hinojosa et al., 2020). However, it should be noted that in differentiated cells they occur at lower concentrations than in undifferentiated cells. Thus, CPF induced signs of cell death such as dilation of the RER cisternae, alteration of the mitochondrial morphology, nucleoli with segregated fibrillary and granular components, a high number of heterophagosomes, and formation of chromatin cumulus in the nucleus. These results are also supported by Park et al. (2015) and Raszewski et al. (2015), who proposed the role of mitochondrial damage in the induction of the caspase cascade, suggesting cell death as one of CPF neurotoxicity mechanisms.

Taking into consideration that the main mechanism of action for CPF is the decrease in AChE activity both in vivo and in vitro (Eaton et al., 2008), the measurement of this enzymatic activity was carried out in our study, obtaining no significant alterations after 24 h of exposure. These results disagree with those obtained in undifferentiated SH-SY5Y cells exposed for 24 h to 0–84 μg/ml CPF, where all concentrations assayed caused a significant reduction in AChE (Hinojosa et al., 2020). A possible explanation for these results would be the effect of CPF on the differentiation process, as the cells are cultivated without serum, or due to the fact that CPF could disrupt neuronal differentiation acting via AChE independent mechanisms, as Todd (2017) reported. In this sense, the differentiation process itself has demonstrated variations in AChE and ACh receptors (Kovalevich and Langford 2013). Furthermore, cell

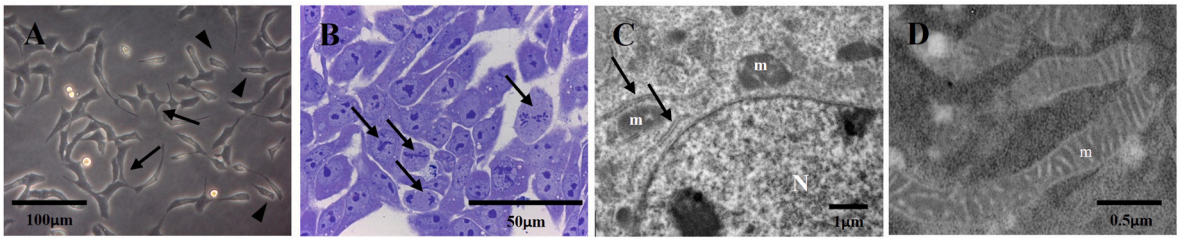

Fig. 5. Morphology of control differentiated SH-SY5Y cells after 24 h of exposure to nutrient medium without serum. Contrast-phase microscopy of a differentiated SH-SY5Y cell culture in normal neuronal growth. Cells with star shape (arrows) present cytoplasmic projections contacting with other cells. Spindle cells with scarce cytoplasmic projections (arrowheads). Bar = 100 μm (A). Semithin sections of cell cultures were stained with toluidine blue. Cells in mitosis processes (arrows). Bar = 50 μm (B). Transmission electronic microscopy of SH-SY5Y cells presenting mitochondria (m), rough endoplasmic reticulum (RER), nucleus (N) and nucleolus (nu). Bar = 1 μm (C). Transmission electronic microscopy of SH-SY5Y cells presenting detailed unaltered mitochondria (m). Bar = 0.5 μm (D). (For interpretation of the references to colour in this figure legend, the reader is referred to the Web version of this article.)

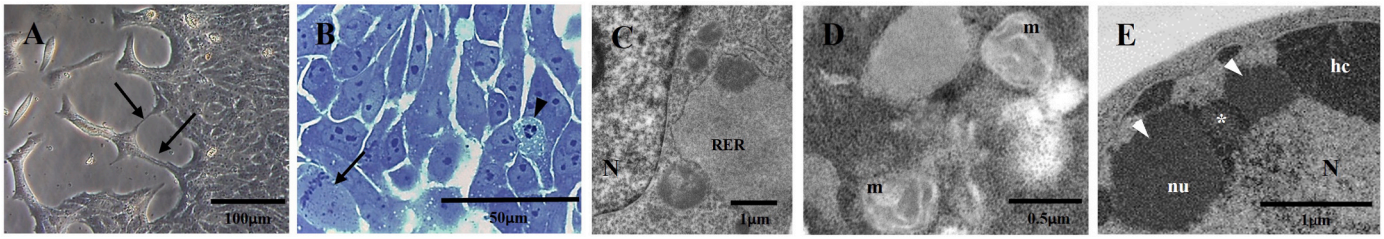

Fig. 6. Morphology of differentiated SH-SY5Y cells after 24 h of exposure to 17 µg/ml CPF. Contrast-phase microscopy of a differentiated SH-SY5Y cell culture with cytoplasmic projections contacting with other cells. Bar = 100 µm (A). Semithin sections of cell cultures were stained with toluidine blue. Cells in mitosis (arrow) and with chromatin condensation (arrowhead). Bar = 50 µm (B). Transmission electronic microscopy of differentiated SH-SY5Y cells presenting dilatations of rough endoplasmic reticulum (RER) (C; Bar = 1 µm) and mitochondrial (m) swelling (D; Bar = 0.5 µm). Transmission electronic microscopy of differentiated SH-SY5Y cells presenting heterochromatin condensation (hc) and the nucleus (N) with altered nucleoli (nu) in segregation processes of the fibrillary (arrowhead) and the granular (asterisk) components. Bar = 1 µm (E). (For interpretation of the references to colour in this figure legend, the reader is referred to the Web version of this article.)

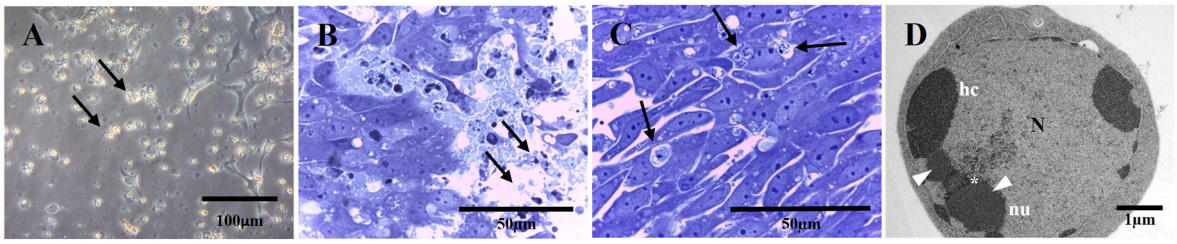

Fig. 7. Morphology of differentiated SH-SY5Y cells after 24 h of exposure to 34 µg/ml CPF. Contrast-phase microscopy of an SH-SY5Y cell culture presenting cell debris (arrows). Bar = 100 µm (A). Semithin sections of cell cultures were stained with toluidine blue. Cell debris (arrows). Bar = 50 µm (B). Semithin sections of cell cultures were stained with toluidine blue. Cells presenting numerous heterophagosomes (arrows). Bar = 50 µm (C). Transmission electronic microscopy of the nucleus (N) of an apoptotic cell presenting heterochromatin condensation in the membrane (hc) and nucleoli (nu) with segregation processes of the fibrillary (arrowhead) and the granular (asterisk) components. Bar = 1 µm (D). (For interpretation of the references to colour in this figure legend, the reader is referred to the Web version of this article.)

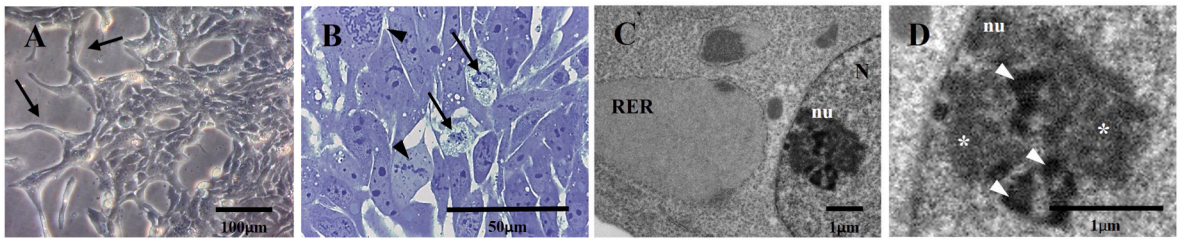

Fig. 8. Morphology of differentiated SH-SY5Y cells after 24 h of exposure to 0.15:17 µg/ml CYN:CPF (v/v). Contrast-phase microscopy of a differentiated SH-SY5Y cell culture presenting cytoplasmic projections contacting with other cells (arrows). Bar = 100 µm (A). Semithin sections of cell cultures were stained with toluidine blue. Cells in mitosis (arrowhead) and apoptosis (arrows) were observed. Bar = 50 µm (B). Transmission electronic microscopy of cells with dilated RER cisternae (RER), nucleus (N) and nucleolus (nu). Bar = 1 µm (C). Transmission electronic microscopy of a detailed nucleolus (nu) with the fibrillary (arrowhead) and the granular (asterisk) components segregated. Bar = 1 µm (D). (For interpretation of the references to colour in this figure legend, the reader is referred to the Web version of this article.)

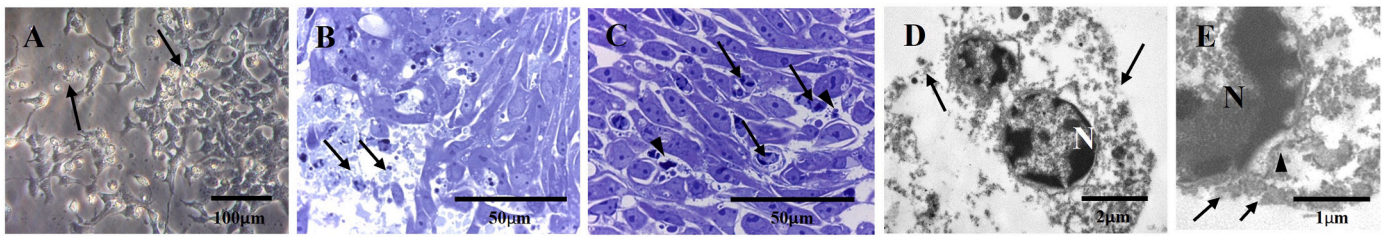

Fig. 9. Morphology of differentiated SH-SY5Y cells after 24 h of exposure to 0.3:34 µg/ml CYN:CPF (v/v). Contrast-phase microscopy of a differentiated SH-SY5Y cell culture presenting numerous cell debris (arrows). Bar = 100 µm (A). Semithin sections of cell cultures were stained with toluidine blue. Cell debris (arrows). Bar = 50 µm (B). Semithin sections of cell cultures were stained with toluidine blue. Cells in different apoptotic stages (arrows) and apoptotic bodies (arrowheads). Bar = 50 µm (C). Transmission electronic microscopy of cells with heterochromatic nuclei (N) and membrane alterations (arrows). Bar = 2 µm (D). Transmission electronic microscopy of a cell and a nucleus (N) with detailed membrane alterations in the nucleus (arrowhead) and cell membrane (arrows) compatible with necrotic processes (arrows). Bar = 1 µm (E). (For interpretation of the references to colour in this figure legend, the reader is referred to the Web version of this article.)

differentiation is associated with changes in metabolism, which could lead to the different responses appreciated between the results obtained in undifferentiated and differentiated cells after the same exposure conditions (Schneider et al., 2011). Variation in gene expression levels before and after differentiation in SH-SY5Y has been observed depending on the type and time of differentiation (Attoff et al. 2020, de Medeiros et al., 2019). In fact, de Medeiros et al. (2019) reported an up-regulation of AChE after differentiation of SH-SY5Y cells, which could allow them to counteract toxic insults more efficiently, explaining the lack of variation of enzyme activity in the present study after exposure to toxicants. This variation in AChE levels has also been reported by Coleman and Taylor (1996), who demonstrated a higher amount of enzyme activity after differentiation of pluripotent P19 stem cells into neurons, have also reported this variation in AChE levels. Concerning the effects of CPF, Jameson et al. (2007) reported an increase in AChE mRNA levels after exposure to CPF in differentiated PC12 cells, which means that it is involved in the toxicity of CPF. However, in differentiated SH-SY5Y, no reduction in enzyme activity was observed.

Having elucidated the toxic effects of CYN (Hinojosa et al. 2019) and CPF alone on differentiated SH-SY5Y cells, the study of the effects of their combination was carried out. These results demonstrated that the CYN + CPF combination was more cytotoxic than the isolated compounds after 48 h of exposure, which agrees with the previous study conducted in undifferentiated SH-SY5Y cells (Hinojosa et al., 2020). To establish what kind of interaction occurs between the two compounds, the isobolograms method was performed by combining the values obtained as EC_{50} (0.3 + 34 μg/ml), $EC_{50}/2$ (0.15 + 17 μg/ml) and $EC_{50}/4$ (0.075 + 8.5 μg/ml) for both CYN and CPF respectively. The response obtained was antagonistic after 24 h exposed to the lowest concentrations, while a synergistic response was detected after being exposed to high concentrations. However, exposure for 48 h produced the contrary effect, causing synergism after exposure to low concentrations and antagonism after exposure to high concentrations. Changes in response after exposure to other toxins mixtures have been reported by Juan-García et al. (2016) in hepatic cells exposed to different combinations of mycotoxins, who found synergism, additivity, and antagonism after 24, 48, and 72 h of exposure, respectively. In this case, the authors attributed these changes to the remaining amount of the main compound of the combination in the medium, which could be a possible explanation in our case. Furthermore, the observed responses are like those obtained in undifferentiated SH-SY5Y exposed to the same toxicants, reporting the same type of response after 48 h of exposure but producing antagonism after all concentrations tested for 24 h. This difference could be due to an increase in cell sensitivity in a more differentiated state, affecting more in differentiated cells when the exposure time is only 24 h. However, another possible explanation could be differences in the ratio of the CYN + CPF mixture selected for both experiments (84/1 in Hinojosa et al. (2020) versus 113/1 in the present study). In this sense, the concentration of CPF against CYN is increased in the current work, with CPF being more cytotoxic than CYN after 24 h of exposure. Furthermore, the metabolic characteristics of the differentiated cell line could also lead to the production of secondary metabolites that may cause changes in cell viability (Todd, 2017). Therefore, different toxicants can cause different responses when exposed alone or in combination, highlighting the importance of studying their toxicity in their natural environment, which is concomitant with more substances. Although these compounds (cyanotoxins and OP) are not usually isolated in nature and their incidence is high, studies that aim to elucidate the effects generated by different pollutants at the same time are scarce.

Regarding the effects on AChE activity caused after exposure to the combination of CYN and CPF, no differences were observed with respect to the control group. Contrary to this, in undifferentiated cells, Hinojosa et al. (2020) reported an intense inhibition of AChE activity after exposure to the mixture for 24 h. There are several possible reasons for this, as explained above (Attoff et al. 2020, de Medeiros et al., 2019; Ellman et al., 1961; Schneider et al., 2011). However, studies on the activity of AChE in differentiated cells are very scarce and nonexistent in our experimental model, despite being one of the most well-known mechanisms of action for OP.

In relation to the morphological observations of the combination on differentiated SH-SY5Y cells, the damage observed was more intense than the one induced by both compounds separately and like the damage shown by the mixture in undifferentiated cells (Hinojosa et al., 2020). However, in this case, apoptotic processes were also observed, which is consistent with the results shown in the flow cytometry assay on apoptosis. These results were also comparable to those shown by Raszewski et al. (2015) and Xu et al. (2017) in this same cell line.

5. Conclusions

Studies carried out in differentiated SH-SY5Y cells demonstrate for the first time a concentration-dependent decrease in cell viability after exposure to CPF alone and in combination with CYN. Furthermore, the interaction between CYN and CPF had an antagonistic response in cell viability after 24 h of exposure to the lowest concentrations, and synergism at the highest, contrary to the results obtained after 48 h of exposure, when the highest concentrations caused antagonism and the lowest led to synergistic effects. However, no changes in AChE activity were observed after exposure to CPF alone or in combination with CYN. Furthermore, the morphological observations revealed an increase in apoptosis with increasing exposure concentration. The combination induced these changes at concentrations lower than those of the compounds alone and, in comparison to undifferentiated cells. Thus, it is important not only to study the toxicity of different toxicants alone, but also to consider how they occur in the natural environment and their possible interaction with other compounds.

Credit author statement

Conceptualization, D. Gutiérrez-Praena, A.I.Prieto, A.M.Cameán and A. Jos; methodology, M.G.Hinojosa, D. Gutiérrez-Praena, S. López, F.J. Moreno; software, M.G.Hinojosa; formal analysis, M.G.Hinojosa D. Gutiérrez-Praena, S. López,; investigation, M.G.Hinojosa; D. Gutiérrez-Praena, S. López, resources, A.M.Cameán and A. Jos; data curation, M.G. Hinojosa; writing—original draft preparation, M.G.Hinojosa; writing—review and editing, D. Gutiérrez-Praena, A.M.Cameán, and A. Jos; visualization, AI. Prieto, A.M.Cameán and A. Jos; project administration, A.M.Cameán and A. Jos; funding acquisition, A.M.Cameán and A. Jos. All authors have read and agreed to the published version of the manuscript.

Ethical statement

No animals or humans were used in the present research paper.

Declaration of competing interest

The authors declare that they have no known competing financial interests or personal relationships that could have appeared to influence the work reported in this paper.

Data availability

Data will be made available on request.

Acknowledgments

The authors want to thank to the Spanish Ministerio de Economía y Competitividad [AGL 2015-64558-R, MINECO/FEDER, Spain, UE], the Spanish Ministerio de Ciencia e Innovación [PID 2019-104890RB-I00, MICINN, Spain] for their financial support. Sergio López also wants to

thank to the "V Plan Propio" of the Universidad de Sevilla [VPPI-US, Sevilla, Spain] for his contract (cofounded by the European Social Fund). The authors also acknowledge the Biology and Microscopy Services of the Centro de Investigación, Tecnología e Innovación from Universidad de Sevilla (CITIUS, Sevilla, Spain) for providing technical assistance. The authors declare no conflict of interests.

References

Ali, U., Syed, J.H., Malik, R.N., Katsoyiannis, A., Li, J., Zhang, G., Jones, K.C., 2014. Organochlorine pesticides (OCPs) in South Asian region: a review. Sci. Total Environ. 476–477, 705–717. https://doi.org/10.1016/j.scitotenv.2013.12.107.

Aswathi, A., Ashok, P., Rajeev, K.S., 2019. Rapid degradation of the organophosphate pesticide – chlorpyrifos by a novel strain of Pseudomonas nitroreducens AR-3. Bio Technol. 292, 122025 https://doi.org/10.1016/j.biortech.2019.122025.

Attoff, K., Johansson, Y., Cediel-Ulloa, A., Lundqvist, J., Gupta, R., Caiment, F., Gliga, A., Forsby, A., 2020. Acrylamide alters CREB and retinoic acid signaling pathways during differentiation of the human neuroblastoma SH-SY5Y cell line. Sci. Rep. 10, 16714 https://doi.org/10.1038/s41598-020-73698-6.

Baltrop, J.A., Owen, T.C., Cory, A.H., Cory, J.G., 1991. 5-(3-carboxymethoxyphenyl)-2-(4,5-dimethylthiazolyl)-3-(4-sulfophenyl)tetrazolium, inner salt (MTS) and related analogs of 3-(4,5-dimethylthiazolyl)-2,5-diphenyltetrazolium bromide (MTT) reducing to purple water-soluble formazans as cell-viability indicators. Bioorg. Med. Chem. Lett. 1, 611–614. https://doi.org/10.1016/S0960-894X(01)81162-8.

Bradford, M.M., 1976. A rapid and sensitive method for the quantitation of microgram quantities of protein utilizing the principle of protein-dye binding. Anal. Biochem. 72, 248–254. https://doi.org/10.1006/abio.1976.9999.

Buratti, F.M., Manganelli, M., Vichi, S., Stefanelli, M., Scardala, S., Testai, E., Funari, E., 2017. Cyanotoxins: producing organisms, occurrence, toxicity, mechanism of action and human health toxicological risk evaluation. Arch. Toxicol. 91, 1049–1130. https://doi.org/10.1007/s00204-016-1913-6.

Carmichael, W.W., Azevedo, S.M., An, J.S., Molica, R.J., Jochimsen, E.M., Lau, S., Rinehart, K.L., Shaw, G.R., Eaglesham, G.K., 2001. Human fatalities from cyanobacteria: chemical and biological evidence for cyanotoxins. Environ. Health Perspect. 109, 663–668. https://doi.org/10.1289/ehp.01109663.

Chiswell, R.K., Shaw, G.R., Eaglesham, G., Smith, M.J., Norris, R.L., Seawright, A.A., Moore, M.R., 1999. Stability of cylindrospermopsin, the toxin from the cyanobacterium, Cylindrospermopsis raciborskii: effect of pH, temperature, and sunlight on decomposition. Environ. Toxicol. 14, 155–161. https://doi.org/10.1002/(SICI)1522-7278.

Coleman, B.A., Taylor, P., 1996. Regulation of acetylcholinesterase expression during neuronal differentiation. J. Biol. Chem. 271, 4410–4416. https://doi.org/10.1074/jbc.271.8.4410.

European Comission, 2020. https://ec.europa.eu/food/plant/pesticides/approval_active_substances/chlorpyrifos_chlorpyrifos-methyl_en.

de Medeiros, L.M., de Bastiani, M., Rico, E.P., Schonhofen, P., Pfaffenseller, B., Wollenhaupt-Aguiar, B., Grun, L., Barbé-Tuana, F., Zimmer, E.R., Castro, M.A., Parsons, R.B., Klamt, F., 2019. Cholinergic differentiation of human neuroblastoma SH-SY5Y cell line and its potential use as an in vitro model for Alzheimer's disease studies. Mol. Neurobiol. 56, 7355–7367. https://doi.org/10.1007/s12035-019-1605-3.

Eaton, D.L., Daroff, R.B., Autrup, H., Bridges, J., Buffler, P., Costa, L.G., Coyle, J., McKhann, G., Mobley, W.C., Nadel, L., Neubert, D., Shulte-Hermann, R., Spencer, P. S., 2008. Review of the toxicology of chlorpyrifos with an emphasis on human exposure and neurodevelopment. Crit. Rev. Toxicol. 38, 1–125. https://doi.org/10.1080/10408440802272158.

Ellman, G.L., Courtney, K.D., Andres, V., Featherstone, R.M., 1961. A new and rapid colorimetric determination of acetylcholin-esterase activity. Biochem. Pharmacol. 7, 88–90. https://doi.org/10.1016/0006-2952(61)90145-9.

European Food Safety Authority, 2019. Statement on the available outcomes of the human health assessment in the context of the pesticides peer review of the active substance chlorpyrifos. EFSA J. 17, 5809. https://doi.org/10.2903/j.efsa.2019.5809.

Falconer, I.R., Humpage, A.R., 2006. Cyanobacterial (blue-green algal) toxins in water supplies: cylindrospermopsins. Environ. Toxicol. 21, 299–304. https://doi.org/10.1002/tox.20194.

Gordon, J., Amini, S., White, M.K., 2013. General overview of neuronal cell culture. Methods Mol. Biol. 1078, 1–8. https://doi.org/10.1007/978-1-62703-640-5_1.

Guzmán-Guillén, R., Lomares, I., Moreno, I.M., Prieto, A.I., Moyano, R., Blanco, A., Cameán, A.M., 2015. Cylindrospermopsin induces neurotoxicity in tilapia fish (Oreochromis niloticus) exposed to Aphanizomenon ovalisporum. Aquat. Toxicol. 161, 17–24. https://doi.org/10.1016/j.aquatox.2015.01.024.

Hassaan, M.A., Nemr, A.E., 2020. Pesticides pollution: classifications, human health impact, extraction and treatment techniques. Egypt J. Aquat. Res. 46, 207–220. https://doi.org/10.1016/j.ejar.2020.08.007.

Hawkins, P.R., Runnegar, M.T., Jackson, A.R., Falconer, I.R., 1985. Severe hepatotoxicity caused by the tropical cyanobacterium (blue-green alga) Cylindrospermopsis raciborskii (Woloszynska) Seenaya and Subba Raju isolated from a domestic water supply reservoir. Appl. Environ. Microbiol. 50, 1292–1295. https://doi.org/10.1128/AEM.50.5.1292-1295.1985.

Hercog, K., Štern, A., Maisanaba, S., Filipič, M., Žegura, B., 2020. Plastics in cyanobacterial blooms—genotoxic effects of binary mixtures of cylindrospermopsin and bisphenols in HepG2 cells. Toxins 12, 219. https://doi.org/10.3390/toxins12040219.

Hinojosa, M.G., Gutiérrez-Praena, D., Prieto, A.I., Guzmán-Guillén, R., Jos, A., Cameán, A.M., 2019a. Neurotoxicity induced by microcystins and cylindrospermopsin: a review. Sci. Total Environ. 668, 547–565. https://doi.org/10.1016/j.scitotenv.2019.02.426.

Hinojosa, M.G., Prieto, A.I., Gutiérrez-Praena, D., Moreno, F.J., Cameán, A.M., Jos, A., 2019b. Neurotoxic assessment of microcystin-LR, cylindrospermopsin and their combination on the human neuroblastoma SH-SY5Y cell line. Chemosphere 224, 751–764. https://doi.org/10.1016/j.chemosphere.2019.02.173.

Hinojosa, M.G., Prieto, A.I., Gutiérrez-Praena, D., Moreno, F.J., Cameán, A.M., Jos, A., 2020. In vitro assessment of the combination of cylindrospermopsin and the organophosphate chlorpyrifos on the human neuroblastoma SH-SY5Y cell line. Ecotoxicol. Environ. Saf. 191, 110222 https://doi.org/10.1016/j.ecoenv.2020.110222.

Hinojosa, M.G., Prieto, A.I., Muñoz-Castro, C., Sánchez-Mico, M.V., Vitorica, J., Cameán, A.M., Jos, A., 2022. Cytotoxicity and effects on the synapsis induced by pure cylindrospermopsin in an E17 embryonic murine primary neuronal culture in a concentration- and time-dependent manner. Toxins 14, 175. https://doi.org/10.3390/toxins14030175.

Huang, X., Cui, H., Duan, W., 2020. Ecotoxicity of chlorpyrifos to aquatic organisms: a review. Ecotoxicol. Environ. Saf. 200, 110731 https://doi.org/10.1016/j.ecoenv.2020.110731.

Jameson, R.R., Seidler, F.J., Slotkin, T.A., 2007. Nonenzymatic functions of acetylcholinesterase splice variants in the developmental neurotoxicity of organophosphates: chlorpyrifos, chlorpyrifos oxon, and diazinon. Environ. Health Perspect. 115, 65–70. https://doi.org/10.1289/ehp.9487.

Jaramillo, S., Lopez, S., Varela, L.M., Rodríguez-Arcos, R., Jimenez, A., Rocío, A., Guillén, R., Muriana, F.J.G., 2010. The flavonol iso-rhamnetin exhibits cytotoxic effects on human colon cancer cells. J. Agric. Food Chem. 58, 10869–10875. https://doi.org/10.1021/jf102669p.

John, E.M., Shaike, J.M., 2015. Chlorpyrifos: pollution and remediation. Environ. Chem. Lett. 13, 269–291. https://doi.org/10.1007/s10311-015-0513-7.

Juan-García, A., Juan, C., Manyes, L., Ruiz, M.J., 2016. Binary and tertiary combination of alternariol, 3-acetyl-deoxynivalenol and 15-acetyl-deoxynivalenol on HepG2 cells: toxic effects and evaluation of degradation products. Toxicol. Vitro 34, 264–273. https://doi.org/10.1016/j.tiv.2016.04.016.

Koly, F.A., Khan, R.A., 2018. Biodegradation of organophosphorous pesticide: chlorpyrifos. A.R.P.G. 5, 8–18. https://doi.org/10.32861/sr.51.8.18.

Kovalevich, J., Langford, D., 2013. Chapter 2: considerations for the use of SH- SY5Y neuroblastoma cells in neurobiology. In: Amini, S., White, M.K. (Eds.), Neuronal Cell Culture, first ed. Springer, New York, pp. 9–22. https://doi.org/10.1007/978-1-62703-640-5.

Lu, M.X., Jiang, W.W., Wang, J.L., Jian, Q., Shen, Y., Liu, X.J., Yu, X.Y., 2014. Persistence and dissipation of chlorpyrifos in Brassica chinensis, lettuce, celery, asparagus lettuce, eggplant, and pepper in a greenhouse. PLoS One 9, e100556. https://doi.org/10.1371/journal.pone.0100556.

Metcalf, J.S., Codd, G.A., 2020. Co-occurrence of cyanobacteria and cyanotoxins with other environmental health hazards: impacts and implications. Toxins 12, 629. https://doi.org/10.3390/toxins12100629.

Park, J.H., Lee, J.E., Shin, I.C., Koh, H.C., 2013. Autophagy regulates chlorpyrifos-induced apoptosis in SH-SY5Y cells. Toxicol. Appl. Pharmacol. 268, 55–67. https://doi.org/10.1016/j.taap.2013.01.013.

Pichardo, S., Jos, A., Zurita, J.L., Salguero, M., Cameán, A.M., Repetto, G., 2007. Acute and subacute toxic effects produced by microcystin-YR on the fish cell lines RTG-2 and PLHC-1. Toxicology 21, 1460–1467. https://doi.org/10.1016/j.tiv.2007.06.012. In Vitro.

Pichardo, S., Cameán, A.M., Jos, A., 2017. In vitro toxicological assessment of cylindrospermopsin: a review. Toxins 9, 402. https://doi.org/10.3390/toxins9120402.

Rahman, H.U.U., Asghar, W., Nazir, W., Sandhu, M.A., Ahmed, A., Khalid, N., 2021. A comprehensive review on chlorpyrifos toxicity with special reference to endocrine disruption: evidence of mechanisms, exposures and mitigation strategies. Sci. Total Environ. 755, 142649 https://doi.org/10.1016/j.scitotenv.2020.142649.

Raszewski, G., Lemieszek, M.K., Łukawski, K., Juszczak, M., Rzeski, W., 2015. Chlorpyrifos and cypermethrin induce apoptosis in human neuroblastoma cell line SH-SY5Y. Basic Clin. Pharmacol. Toxicol. 116, 158–167. https://doi.org/10.1111/bcpt.12285.

Santillo, M.F., Liu, Y., 2015. A fluorescence assay for measuring acetylcholinesterase activity in rat blood and a human neuro-blastoma cell line (SH-SY5Y). J. Pharmacol. Toxicol. Methods 76, 15–22. https://doi.org/10.1016/j.vascn.2015.07.00.

Schneider, L., Giordano, S., Zelickson, B.R., Johnson, M.S., Benavides, G.A., Ouyang, X., Fineberg, N., Darley-Usmar, V.M., Zhang, J., 2011. Differentiation of SH-SY5Y cells to a neuronal phenotype changes cellular bioenergetics and the response to oxidative stress. Free Radic. Biol. Med. 51, 2007–2017. https://doi.org/10.1016/j.freeradbiomed.2011.08.030.

Singh, A.K., Singh, P.P., Tripathi, V., Verma, H., Singh, S.K., Srivastava, A.K., Kumar, A., 2018. Distribution of cyanobacteria and their interactions with pesticides in paddy field: a comprehensive review. J. Environ. Manag. 224, 361–375. https://doi.org/10.1016/j.jenvman.2018.07.039.

Tatay, E., Meca, G., Font, G., Ruiz, M.J., 2014. Interactive effects of zearalenone and its metabolites on cytotoxicity and metabolization in ovarian CHO-K1 cells. Toxicol. Vitro 28, 95–103. https://doi.org/10.1016/j.tiv.2013.06.025.

Tiffany-Castiglioni, E., Venkatraj, V., Qian, Y., Wild, J.R., 2006. In vitro models for testing organophosphate-induced neurotoxicity and remediation. In: Gupta, R. (Ed.),

Toxicology of Organophosphate & Carbamate Compounds, first ed. Elsevier, Texas, pp. 315–337. https://doi.org/10.1016/B978-012088523-7/50023-5.
Todd, S.W., 2017. Effects of Continuous Exposure of SH-Sy5y Neuroblastoma Cells to Chlorpyrifos on Neuronal Differentiation: Implications for Neurotoxicity. Ph.D., University of Maryland.
Vermes, I., Haanen, C., Steffens-Nakken, H., Reutelingsperger, C., 1995. A novel assay for apoptosis Flow cytometric detection of phosphatidylserine expression on early apoptotic cells using fluorescein labelled Annexin V. J. Immunol. Methods 184, 39–51. https://doi.org/10.1016/0022-1759(95)00072-I.
Walker, C.H., 1998. The use of biomarkers to measure the interactive effects of chemicals. Ecotoxicol. Environ. Saf. 40, 65–70. https://doi.org/10.1006/eesa.1998.1643.
Wang, Z., Zhang, J., Li, E., Zhang, L., Wang, Z., Song, L., 2017. Combined toxic effects and mechanisms of microsystin-LR and copper on Vallisneria natans (Lour.) Hara seedlings. J. Hazard Mater. 328, 108–116. https://doi.org/10.1016/j.jhazmat.2016.12.059.
Watts, M., 2012. Chlorpyrifos as a Possible Global POP. Pesticide Action Network North America, Oakland, CA. https://www.pan-europe.info/old/News/PR/121009_Chlorpyrifos_as_POP_final.pdf.
Worek, F., Widmann, R., Knopff, O., Szinicz, L., 1998. Reactivating potency of obidoxime, pralidoxime, HI 6 and HL 7 in human erythrocyte acetylcholinesterase inhibited by highly toxic organophosphorus compounds. Arch. Toxicol. 72, 237–243. https://doi.org/10.1007/s002040050495.
World Health Organization, 2020. Cyanobacterial Toxins: Cylindrospermopsins. Background Document for Development of WHO Guidelines for Drinking-Water Quality and Guidelines for Safe Recreational Water Environments.
Wörmer, L., Huerta-Fontela, M., Cirés, S., Carrasco, D., Quesada, A., 2010. Natural photodegradation of the cyanobacterial toxins microcystin and cylindrospermopsin. Environ. Sci. Technol. 44, 3002–3007. https://doi.org/10.1021/es9036012.
Xu, M.Y., Wang, P., Sun, Y.J., Yang, L., Wu, Y.J., 2017. Joint toxicity of chlorpyrifos and cadmium on the oxidative stress and mitochondrial damage in neuronal cells. Food Chem. Toxicol. 103, 246–252. https://doi.org/10.1016/j.fct.2017.03.013.
Yang, Y., Yu, G., Chen, Y., Jia, N., Li, R., 2021. Four decades of progress in cylindrospermopsin research: the ins and outs of a potent cyanotoxin. J. Hazard. Marter. 406, 124653 https://doi.org/10.1016/j.jhazmat.2020.124653.
Yurumez, Y., Durukan, P., Yavuz, Y., Ikizceli, I., Avsarogullari, L., Ozkan, S., Akdur, O., Ozdemir, C., 2007. Acute organophosphate poisoning in university hospital emergency room patients. Intern. Med. 46, 965–969. https://doi.org/10.2169/internalmedicine.46.6304.
Zurich, M.G., Honegger, P., Schilter, B., Costa, L.G., Monnet-Tschudi, F., 2004. Involvement of glial cells in the neurotoxicity of parathion and chlorpyrifos. Toxicol. Appl. Pharmacol. 201, 97–104. https://doi.org/10.1016/j.taap.2004.05.003.